J|A|C|S
ARTICLES

Published on Web 01/15/2009

Transition-State Geometry Measurements from ^{13}C Isotope Effects. The Experimental Transition State for the Epoxidation of Alkenes with Oxaziridines

Jennifer S. Hirschi,* Tetsuya Takeya,† Chao Hang, and Daniel A. Singleton*

Department of Chemistry, Texas A&M University, College Station, Texas 77842

Received November 11, 2008; E-mail: jennifer.hirschi@gmail.com; singleton@mail.chem.tamu.edu

Abstract: We here suggest and evaluate a methodology for the measurement of specific interatomic distances from a combination of theoretical calculations and experimentally measured ^{13}C kinetic isotope effects. This process takes advantage of a broad diversity of transition structures available for the epoxidation of 2-methyl-2-butene with oxaziridines. From the isotope effects calculated for these transition structures, a theory-independent relationship between the C−O bond distances of the newly forming bonds and the isotope effects is established. Within the precision of the measurement, this relationship in combination with the experimental isotope effects provides a highly accurate picture of the C−O bonds forming at the transition state. The diversity of transition structures also allows an evaluation of the Schramm process for defining transition-state geometries on the basis of calculations at nonstationary points, and the methodology is found to be reasonably accurate.

Introduction

Spectroscopic methods can be used to delineate ground-state structures, even when these structures are very short-lived, but only very rarely can spectroscopy be applied to define transition-state geometries. Rather, transition states are characterized indirectly, invariably by some form of kinetics experiment. This is very limiting, but not infinitely so; many forms of kinetics observations resolve qualitative features of transition-state structures. The quantitative experimental characterization of transition-state geometries remains largely out of reach.[1]

Kinetic isotope effects (KIEs) have long been used as a qualitative measure of transition-state geometry or as a semi-quantitative measure of transition-state bond orders.[2] The potential for a more detailed geometrical interpretation arose with Hess and Schaad's first comparisons of experimental and ab initio-predicted isotope effects,[3] though this was hampered by doubt in the predictions.[3a,4] An advance came when Houk and Singleton found that conventional transition-state theory with a one-dimensional tunneling correction could predict KIEs very well,[5] particularly heavy-atom KIEs, provided that the calculated transition-state geometry is accurate and that the reaction does not involve a hydrogen transfer.[6] The prediction of KIEs can be complicated by the substantial involvement of dynamics, multidimensional tunneling, variational transition-state effects, and other specialized effects; however, use of more complex theoretical treatments can often account for these effects. [7] Complications also arise when solvation plays a significant role in the reaction, such as in reactions involving charge separation, where solvent effects can be difficult to model accurately. Despite expected limitations, a close correspondence between predicted and experimental KIEs has been observed in many cases, and this has been interpreted as supporting the accuracy of the calculated transition structures.[5,6,8,9]

Schramm has developed a method for defining the transition states of enzymatic reactions on the basis of KIE measurements. In this method, a systematic search of constrained geometries is undertaken in order to identify structures that lead to correct

† Deceased on June 19, 2006.

(1) For an exception, see: Wenthold, P. G.; Hrovat, D. A.; Borden, W. T.; Lineberger, W. C. *Science* **1996**, *272*, 1456–1459.
(2) (a) Bigeleisen, J.; Wolfsberg, M. *Adv. Chem. Phys.* **1958**, *1*, 16–76. (b) Melander, L.; Saunders, W. H., Jr. *Isotope Effects on Reaction Rates*; Wiley-Interscience: New York, 1980. (c) O'Ferrall, R. A. M. *J. Chem. Soc. B* **1970**, 785–790. (d) Katz, A. M.; Saunders, W. H., Jr. *J. Am. Chem. Soc.* **1969**, *91*, 4469–4472. (e) Streitwieser, A., Jr.; Jagow, R. H.; Suzuki, S. *J. Am. Chem. Soc.* **1958**, *80*, 2326–2332.
(3) (a) Hess, B. A., Jr.; Schaad, L. J.; Pancir, J. *J. Am. Chem. Soc.* **1985**, *107*, 149–154. (b) Baldwin, J. E.; Reddy, V. P.; Hess, B. A., Jr.; Schaad, L. J. *J. Am. Chem. Soc.* **1988**, *110*, 8554–8555.
(4) Lu, D.-h.; Maurice, D.; Truhlar, D. G. *J. Am. Chem. Soc.* **1990**, *112*, 6206–6214.
(5) Beno, B. R.; Houk, K. N.; Singleton, D. A. *J. Am. Chem. Soc.* **1996**, *118*, 9984–9985.
(6) Meyer, M. P.; DelMonte, A. J.; Singleton, D. A. *J. Am. Chem. Soc.* **1999**, *121*, 10865–10874.
(7) (a) Singleton, D. A.; Hang, C.; Szymanski, M. J.; Greenwald, E. E. *J. Am. Chem. Soc.* **2003**, *125*, 1176–1177. (b) Ussing, B. R.; Hang, C.; Singleton, D. A. *J. Am. Chem. Soc.* **2006**, *128*, 7594–7607. (c) Nowlan, D. T., III; Singleton, D. A. *J. Am. Chem. Soc.* **2005**, *127*, 6190–6191. (e) Lin, H.; Zhao, Y.; Ellingson, B. A.; Pu, J.; Truhlar, D. G. *J. Am. Chem. Soc.* **2005**, *127*, 2830–2831. (f) Ellingson, B. A.; Pu, J.; Lin, H.; Zhao, Y.; Truhlar, D. G. *J. Phys. Chem. A* **2007**, *111*, 11706–11717. (g) Ellingson, B. A.; Truhlar, D. G. *J. Am. Chem. Soc.* **2007**, *129*, 12765–12771. (h) Garrett, B. C.; Truhlar, D. G.; Bowman, J. M.; Wagner, A. F.; Robie, D.; Arepalli, S.; Presser, N.; Gordon, R. J. *J. Am. Chem. Soc.* **1986**, *108*, 3515–3516.
(8) For some other examples, see: (a) Singleton, D. A.; Merrigan, S. R.; Liu, J.; Houk, K. N. *J. Am. Chem. Soc.* **1997**, *119*, 3385–3386. (b) DelMonte, A. J.; Haller, J.; Houk, K. N.; Sharpless, K. B.; Singleton, D. A.; Strassner, T.; Thomas, A. A. *J. Am. Chem. Soc.* **1997**, *119*, 9907–9908. (c) Keating, A. E.; Merrigan, S. R.; Singleton, D. A.; Houk, K. N. *J. Am. Chem. Soc.* **1999**, *121*, 3933–3938. (d) Singleton, D. A.; Wang, Z. *J. Am. Chem. Soc.* **2005**, *127*, 6679–6685.
(9) For an example highlighting a limitation of this process, see: Singleton, D. A.; Hang, C. *J. Org. Chem.* **2000**, *65*, 7554–7560.

10.1021/ja8088636 CCC: $40.75

predictions of the experimental KIEs.[10] The use of such constrained geometries notably compromises the frequency calculations on which the KIE predictions rely, so the theoretical rigor of the Schramm process is questionable. Nonetheless, it is extraordinarily successful, having been used to design some of the most powerful enzyme inhibitors known.[11]

The precise interpretation of a KIE in terms of transition-state geometry requires that the KIE in fact be directly related to a transition-state geometrical parameter. Theory does not obviously require this; KIEs are a function of transition-state and starting-material vibrational frequencies that are themselves a complex function of the geometry. Several studies in the literature have probed the relationship between transition-state geometry and KIEs.[12] In an incisive series of studies, Jensen and co-workers explored the relationship between transition-state geometries and H/D KIEs in S_N2 and E2 reactions.[12b−e,g,i] They notably observed a smooth relationship between bond orders and primary isotope effects after compensation for complicating factors, though the relationship was flat for a broad range of bond orders, largely precluding a specific geometrical interpretation of primary isotope effects. The lore in the isotope-effect area is that secondary H/D KIEs are closely related to transition-state geometry, but Jensen and co-workers' studies show that the correlation of the two is complex when it exists at all. In four transition structures at varying calculational levels for the Claisen rearrangement, there was no trend in geometry versus predicted heavy-atom KIEs, and only geometrically extreme transition states could be completely excluded.[6] These observations suggest a limited "resolution" for KIEs in determining transition-state geometry. In contrast, we show here that a precise and detailed geometrical interpretation of KIEs is possible, and we identify an error to be avoided in relating KIEs to geometry.

To probe the relationship of the ^{13}C isotope effects to particular features of the transition-state geometry, we needed a series of transition structures with varying geometries. Epoxidations of alkenes with oxaziridines (eq 1) provided a unique opportunity in this regard. Experimental studies of these

(1)

reactions have been interpreted as favoring both planar and spiro transition states.[13−15] A concerted mechanism has largely been assumed on the basis of the stereospecifity of the epoxidation, though stepwise mechanisms have also been proposed in special cases.[16,17] Early theoretical studies (RHF/STO-3G) by Bach and Wolber[18] on the epoxidation of alkenes with oxaziridines predicted a planar transition structure. Later MP2 calculations predicted a late, spiro, synchronous transition structure,[19] and the most recent B3LYP calculations by Houk et al.[20] predicted a spiro but highly asynchronous transition-state geometry. In each case, the calculational model was highly simplified compared with experimentally successful reactions, and we will see here that none of the calculations accurately describe a typical experimental reaction. For our purposes, the complexities inherent in the epoxidation of alkenes by oxaziridines afford a diverse array of structures that arise from varying substitutions, conformations, and orientations of the oxaziridine. The analysis of the KIEs for these structures provides the basis for their geometric interpretation. This study also allows a detailed probe of the Schramm process for defining transition-state geometries.

Results and Discussion

Experimental Isotope Effects. A qualitative question regarding additions to alkenes is whether there is synchronous or asynchronous formation of the bonds to the olefinic carbons. Since unsymmetrically substituted alkenes necessarily react via unsymmetrical transition states, the question of synchroneity is only strictly meaningful with symmetrically substituted alkenes. However, symmetrical alkenes must exhibit symmetrical isotope effects as a result of averaging, so probes of transition-state synchroneity have focused on "slightly unsymmetrical" reactants.[8,21] Here, the epoxidation of 2-methyl-2-butene was chosen for study. The epoxidation of 2-methyl-2-butene with **1** proceeds slowly at room temperature and affords epoxide **2** quantitatively when an excess of **1** is used.

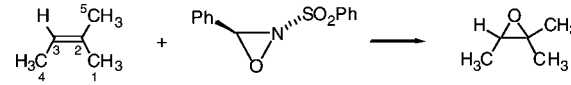

1 **2**

The ^{13}C KIEs for this reaction were determined combinatorially by NMR methodology at natural abundance.[22] Oxidations of 2-methyl-2-butene on a 0.15 mol scale with limiting **1** in chloroform at room temperature were taken to 77 ± 3% and 78 ± 3% conversion. The unreacted alkene was reisolated by successive distillations and then analyzed by ^{13}C NMR in comparison with a standard not subjected to the reaction conditions. The changes in isotopic composition were calculated using the C5 methyl carbon as an "internal standard" under the

(10) (a) Horenstein, B. A.; Parkin, D. W.; Estupinan, B.; Schramm, V. L. *Biochemistry* **1991**, *30*, 10788–10795. (b) Horenstein, B. A.; Schramm, V. L. *Biochemistry* **1993**, *32*, 7089–7097. (c) Also see ref 12b, which employs a similar process.

(11) (a) Singh, V.; Lee, J. E.; Nunez, S.; Howell, P. L.; Schramm, V. L. *Biochemistry* **2005**, *44*, 11647–11659. (b) Miles, R. W.; Tyler, P. C.; Furneaux, R. H.; Bagdassarian, C. K.; Schramm, V. L. *Biochemistry* **1998**, *37*, 8615–8621. (c) Taylor, E. A.; Clinch, K.; Kelly, P. M.; Li, L.; Evans, G. B.; Tyler, P. C.; Schramm, V. L. *J. Am. Chem. Soc.* **2007**, *129*, 6984–6985.

(12) (a) Owczarek, E.; Kwiatkowski, W.; Lemieszewski, M.; Mazur, A.; Rostkowski, M.; Paneth, P. *J. Org. Chem.* **2003**, *68*, 9302–9310. (b) Glad, S. S.; Jensen, F. *J. Am. Chem. Soc.* **1997**, *119*, 227–232. (c) Glad, S. S.; Jensen, F. *J. Org. Chem.* **1997**, *62*, 253–260. (d) Nielsen, P. A.; Glad, S. S.; Jensen, F. *J. Am. Chem. Soc.* **1996**, *118*, 10577–10583. (e) Jensen, F. *J. Am. Chem. Soc.* **1995**, *117*, 7487–7492. (f) Wiest, O.; Houk, K. N.; Black, K. A.; Thomas, B., IV *J. Am. Chem. Soc.* **1995**, *117*, 8594–8599. (g) Glad, S. S.; Jensen, F. *J. Am. Chem. Soc.* **1994**, *116*, 9302–9310. (h) Poirier, R. A.; Wang, Y.; Westaway, K. C. *J. Am. Chem. Soc.* **1994**, *116*, 2526–2533. (i) Glad, S. S.; Jensen, F. *J. Chem. Soc., Perkin Trans. 2* **1994**, *4*, 871–876. (j) Wilkie, J.; Williams, I. H. *J. Am. Chem. Soc.* **1992**, *114*, 5423–5425. (k) Wolfe, S.; Kim, C.-K. *J. Am. Chem. Soc.* **1991**, *113*, 8056–8061.

(13) Davis, F. A.; Harakal, M. E.; Awad, S. B. *J. Am. Chem. Soc.* **1983**, *105*, 3123–3126.

(14) (a) Baumstark, A. L.; McCloskey, C. J. *Tetrahedron Lett.* **1987**, *28*, 3311–3314. (b) Tu, Y.; Wang, Z.-X.; Shi, Y. *J. Am. Chem. Soc.* **1996**, *118*, 9806–9807.

(15) Anderson, D. R.; Woods, K. W.; Beak, P. *Org. Lett.* **1999**, *1*, 1415–1417.

(16) Mithani, S.; Drew, D. M.; Rydberg, E. H.; Taylor, N. J.; Mooibroek, S.; Dmitrienko, G. I. *J. Am. Chem. Soc.* **1997**, *119*, 1159–1160.

(17) Yang, D.; Zhang, C.; Wang, X.-C. *J. Am. Chem. Soc.* **2000**, *122*, 4039–4043.

(18) Bach, R. D.; Wolber, G. J. *J. Am. Chem. Soc.* **1984**, *106*, 1410–1415.

(19) Bach, R. D.; Andres, J. *J. Org. Chem.* **1992**, *57*, 613–618.

(20) Houk, K. N.; Liu, J.; DeMello, N. C.; Condroski, K. R. *J. Am. Chem. Soc.* **1997**, *119*, 10147–10152.

(21) Gajewski, J. J.; Peterson, K. B.; Kagel, J. R.; Huang, Y. C. J. *J. Am. Chem. Soc.* **1989**, *111*, 9078–9081.

(22) Singleton, D. A.; Thomas, A. A. *J. Am. Chem. Soc.* **1995**, *117*, 9357–9358.

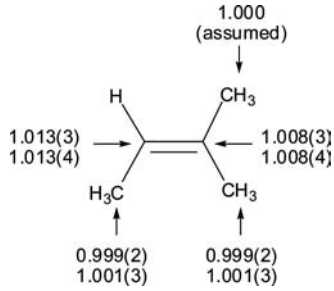

Figure 1. Experimental ^{13}C KIEs ($k_{^{12}C}/k_{^{13}C}$) at 25 °C for the epoxidation of 2-methyl-2-butene with **1**. The two sets of KIEs refer to two independent experiments, with each result based on the average of six measurements. Standard deviations in the last digit are shown in parentheses.

assumption that its isotopic composition does not change during the reaction.[23] From the changes in isotopic composition, the KIEs were calculated as previously described.[22] The results are summarized in Figure 1.

Theoretical Structures. As will be described below, a variety of calculational methods were explored in these reactions, but the majority of the theoretical structures were derived from B3LYP calculations using a 6-31+G** basis set.[24] This combination was supported by comparison of the transition-structure geometry with a fully optimized CCSD(T)/6-31+G** structure for the parent reaction (see the Supporting Information) along with the prediction of a reasonably accurate barrier versus experimental observations. This methodology was also ultimately supported by the isotope effect observations.

From a systematic search on the reaction of 2-methyl-2-butene with 2-(methylsulfonyl)oxaziridine, followed by more selective searches on reactions with *trans*- and *cis*-3-phenyl-2-methanesulfonyloxaziridine, a total of 18 transition structures were located in B3LYP calculations using a 6-31+G** basis set. All of the geometries were reoptimized using a PCM implicit solvent model to explore the effects of solvent on the stabilization of the transition state. Eight 2-(methylsulfonyl)oxaziridine-based transition structures were also reoptimized using an Onsager solvent model, leading to a total of 44 transition structures for the calculation of isotope effects as described below (see the Supporting Information).

The four lowest-energy transition structures located with 2-(methylsulfonyl)oxaziridine were structures **3**−**6**, which are shown in Figure 2; the rest are shown in the Supporting Information. The multiplicity of structures arises from the possibility of (1) a syn or anti arrangement of the methylene group of the oxaziridine and the cis methyl groups of the alkene, (2) an orientation of the methanesulfonyl group toward either the more- or less-substituted end of the alkene, and (3) variation in the rotational orientation of the methanesulfonyl group.

In the gas-phase structures, the oxygens of the methanesulfonyl group are partially associated with hydrogens of the alkene methyl groups. Since this charge−charge interaction would be greatly overemphasized relative to the solution chemistry, **3**−**6** were reoptimized using both the Onsager and PCM solvation models. This led to significant changes in the structures: in the presence of solvent, the sulfonyl oxygen···methyl hydrogen

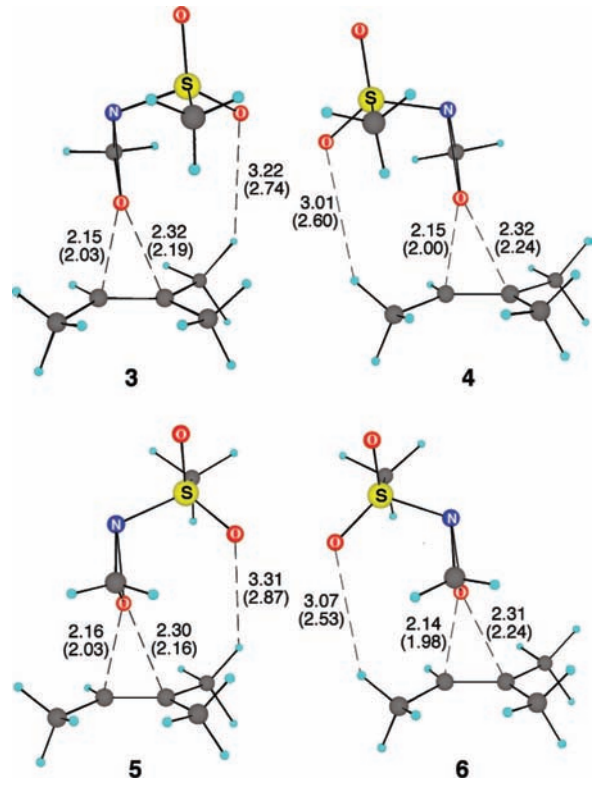

Figure 2. The four lowest-energy B3LYP/6-31+G** transition structures for the epoxidation of 2-methyl-2-butene with 2-(methylsulfonyl)oxaziridine. Distances (Å) in parentheses are from gas-phase optimizations, and distances without parentheses are from optimizations using a PCM implicit solvation model.

distances are increased, and there is a general shift toward an earlier transition structure with more synchronous formation of the epoxide C−O bonds. Solvent has a greater effect on the energetics of transition structures with two sulfonyl oxygen−methyl interactions (see structures **3** and **5** as well as structures in the Supporting Information), resulting in an increase in the relative energies of these isomers. Solvent has previously been shown to have a substantial effect on the energetics of a fluorine−hydrogen interaction in epoxidations with fluorinated dioxiranes.[25] We would suggest in general that great care should be taken in interpreting heteroatom···H−C interactions from gas-phase calculations.

The free energies of all eight of the solvent-optimized transition structures are within 2.2 kcal/mol (PCM solvent model) of the lowest-energy structure **3**. The multitude of similar-energy structures makes obvious the difficulty of obtaining high asymmetric induction in these reactions. The free-energy barrier calculated by treating the experimental concentrations as the standard state is 22.2−24.4 kcal/mol (with a 15.3−17.4 kcal/mol enthalpic barrier), in line with reactions that proceed slowly at room temperature.

The four transition structures obtained for the reaction of *trans*-3-phenyl-2-methanesulfonyloxaziridine, depicted as **7**−**10** in Figure 3, are analogues of isomers **3**−**6** (see the Supporting Information for complete structures with stereo views). The presence of the phenyl group is predicted to notably increase the free-energy barrier for the reaction in solvent by 4.7 kcal/mol. The free energies of all of the *trans*-3-phenyl-2-methane-

(23) The predicted KIEs for the methyl carbons ranged from 0.998 to 1.000 for 69 different transition structures calculated using B3LYP with various basis sets in the gas phase and with various solvent models.

(24) (a) Frisch, M. J.; et al. *Gaussian 03*, revision C.02; Gaussian, Inc: Wallingford, CT, 2004. (b) See the Supporting Information for full details regarding the calculational methods employed.

(25) Armstrong, A.; Washington, I.; Houk, K. N. *J. Am. Chem. Soc.* **2000**, *122*, 6297–6298.

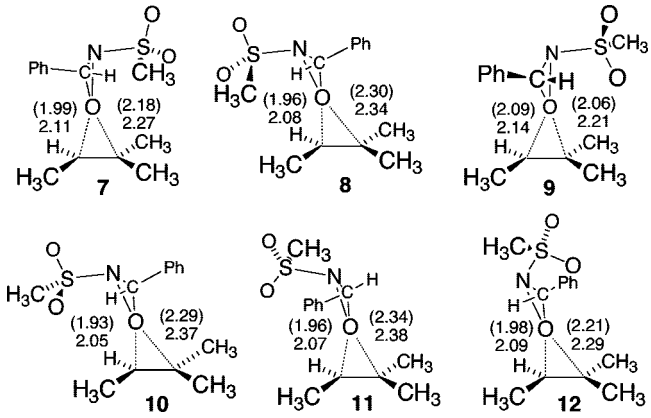

Figure 3. B3LYP/6-31+G** transition structures for the epoxidation of 2-methyl-2-butene with *trans*-3-phenyl-2-methanesulfonyloxaziridine (**7**−**10**) and *cis*-3-phenyl-2-methanesulfonyloxaziridine (**11** and **12**). Distances (Å) in parentheses are from gas-phase optimizations, and distances without parentheses are from optimizations using a PCM implicit solvent model.

sulfonyloxaziridine isomers are within 1.5 kcal/mol of lowest-energy structure **7**. Transition structures **11** and **12** were located for the reaction of *cis*-3-phenyl-2-methanesulfonyloxaziridine; these structures are analogues of **3** and **4**, respectively (see the Supporting Information for additional structures). The starting cis oxaziridine is predicted to be less stable than the trans isomer by 6.7 kcal/mol. This higher energy is not expected to afford greater reactivity; transition structure **12,** the cis structure with the lowest free energy, is 7.2 kcal/mol higher in energy than best trans structure **7**, making the free-energy barrier (activation energy) for the reaction of the cis oxaziridine 0.5 (0.8) kcal/mol higher than that for the trans isomer. Yang et al.[17] have proposed that the cis oxaziridine acts as the oxidant in the epoxidation of alkenes with the in situ-generated 3-phenyl-2-methanesulfonyloxaziridine. However, the current study suggests that the cis isomers play only a minor role in the reaction, since these transition structures on average have much higher barriers than the trans congeners (1.5 kcal/mol on average).

All of the epoxidation transition structures are best described as spiro; however, the asynchroneity of the two newly forming C−O bonds varies considerably. In the absence of obvious steric interactions, a nearly synchronous transition structure seems to be preferred, as shown in **7** and **9**. Steric interactions between the phenyl group of the oxaziridine and the methyl groups of the alkene, as in structures **8** and **10**, cause the geometry to distort to highly asynchronous C−O bond formation. Unsurprisingly, the sterically encumbered cis structures distort readily to minimize steric interactions (compare **7** with **11** and structures in the Supporting Information).

Predicted Isotope Effects. The isotope effects for each of the 44 transition structures were calculated from conventional transition-state theory by the method of Bigeleisen and Mayer[26] from the scaled theoretical vibrational frequencies,[27] and tunneling corrections were applied using a one-dimensional infinite

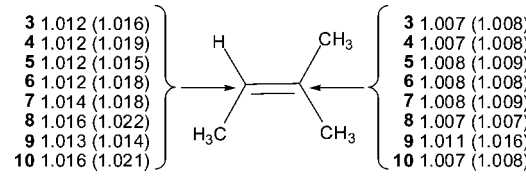

Figure 4. Predicted ^{13}C KIEs (k_{12C}/k_{13C}) for the olefinic carbons of transition-state structures **3**−**10** for the epoxidation of 2-methyl-2-butene catalyzed by 2-(methylsulfonyl)oxaziridine (**3**−**6**) and *trans*-3-phenyl-2-methanesulfonyloxaziridine (**7**−**10**). Predicted KIEs from gas-phase optimizations are shown in parentheses, and KIEs from optimizations with an implicit PCM solvent model are shown without parentheses.

parabolic barrier model.[28] Such KIE predictions have proven to be highly accurate in reactions not involving hydrogen transfer, so long as the calculation accurately depicts the mechanism and transition-state geometry.[5,6,8] The 88 predicted isotope effects for the olefinic carbons are summarized in the Supporting Information.

In analogy with previous studies, a comparison with experimental values to prune the theoretical structures and evaluate the accuracy of the best structures was applied. The predicted KIEs for **3**−**10** are shown in Figure 4. Though most of the structures calculated without using the implicit solvation model (displayed in parentheses) lead to isotope effects that do not match well with the experimental values in Figure 1, all eight structures calculated using the implicit PCM solvation model give KIEs within the error of the experimental measurements. Structures involving 2-(methylsulfonyl)oxaziridine (**3**−**6**) correctly lead to excellent preditions of the experimental KIEs, despite the simplicity of the calculational model. For the *trans*-3-phenyl-2-methanesulfonyloxaziridine series of structures (**7**−**10**), which more closely resemble the experimental system, the lowest-energy transition structure **7** gives particularly good agreement with experiment. The predicted KIEs for structures **8**−**10** lie on the edge of experimental error; however, after allowing for two independent experimental measurements, the 95% confidence range does not include the predicted KIEs for **8**−**10**. The highly asynchronous structure **8** is similar in energy to **7**, but the relative energies are sufficiently unreliable that the calculations do not exclude **7** as the predominant contributor to the transition-state ensemble, as suggested by the KIEs.

The arguably best theoretical structure **7** is consistent with the spiro transition state proposed by Bach and Andres;[19] however, the model is much earlier and more synchronous than previously predicted by Houk et al.[20] for the reaction of ethylene with oxaziridine. The current study demonstrates the importance of including all of the alkene substituents in developing an accurate theoretical model.[29] A solvent model is also necessary in systems involving oxygen···H−C interactions, which are overestimated in the gas-phase.

Geometries from Isotope Effects. From the diverse set of theoretical structures, we can examine in detail the connection between transition-state geometry and KIEs. This analysis also provides a unique opportunity to evaluate the accuracy of the Schramm process in predicting transition-state geometries.

(26) (a) Bigeleisen, J.; Mayer, M. G. *J. Chem. Phys.* **1947**, *15*, 261–267. (b) Wolfsberg, M. *Acc. Chem. Res.* **1972**, *5*, 225–233. (c) It should be noted that the Bigeleisen method fully allows for free energy but is less subject to errors in low frequencies than a direct calculation of KIEs from activation free energies (see ref 31 and the Supporting Information).

(27) The calculations used the program QUIVER: Saunders, M.; Laidig, K. E.; Wolfsberg, M. *J. Am. Chem. Soc.* **1989**, *111*, 8989–8994.

(28) Bell, R. P. *The Tunnel Effect in Chemistry*; Chapman & Hall: London, 1980; pp 60−63.

(29) An optimized transition structure of the reaction of ethylene with oxazaridine using a PCM solvent model results in a highly asynchronous structure with bond distances of 1.78 and 2.22 Å and predicted ^{13}C KIEs of 1.023 and 1.010, respectively, which is inconsistent with experimental observations.

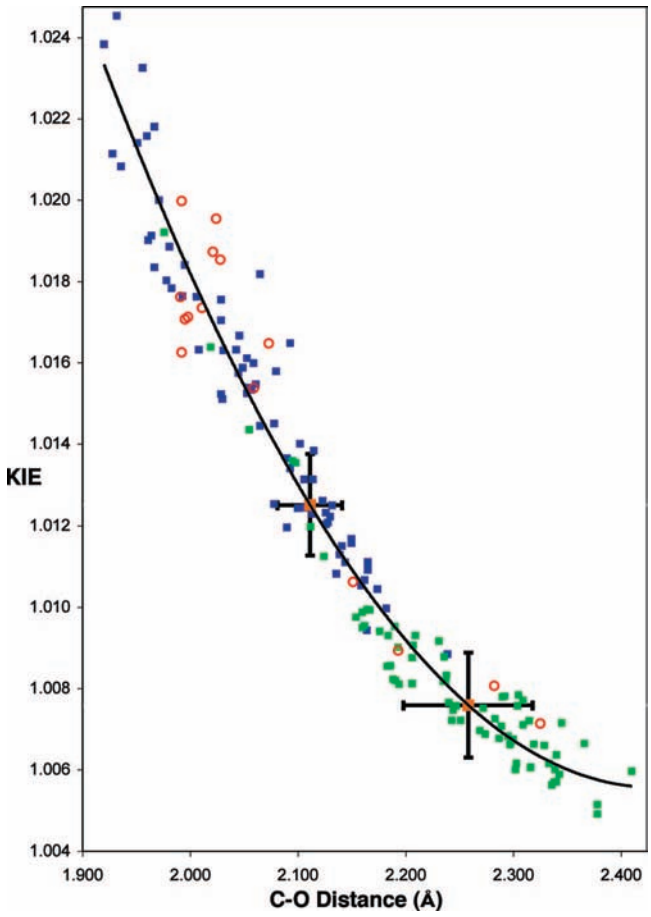

Figure 5. Relationship between ^{13}C KIEs (k_{12C}/k_{13C}) and C−O bond distances for the newly forming olefinic bonds in the oxaziridination of 2-methyl-2-butene. Predictions were calculated for C3 (blue squares) and C2 (green squares) from a variety of B3LYP-optimized structures. The solid line is a quadratic fit to all of the B3LYP points. Predictions from other theoretical methods with reasonable energetic barriers (BPW91, B3PW91, BP86, MPW3LYP, MPWLYP1M, MPW1B95, TPSSKCIS, PBE1KCIS) are also depicted (red open circles). Absolute experimental KIEs of 1.0125 and 1.0075 (orange squares) and their uncertainties, as obtained from a combination of experimental measurements, are also shown. The *absolute* experimental KIEs (rather than the *relative* experimental KIEs in Figure 1) are represented here to facilitate comparison with the *absolute* predicted values. Absolute experimental values were determined as the product of each experimental measurement and the average of all of the predicted KIEs at C5 (0.9994).

To obtain a quantitative geometrical interpretation of the isotope effects, the relationship between the predicted KIEs and the C−O bond distances for the newly forming C−O bonds was examined for the various transition structures. Figure 5 shows a plot of the predicted ^{13}C olefinic KIEs for the calculated structures versus the corresponding C−O bond distances. The significant observation in this plot is the close relationship of the predicted KIEs with the C−O distance across a wide variety of structures.

This is profound. All 70 structures[30] have $3N - 6$ vibrational frequencies that factor into the isotope effect calculation, and the 70 structures differ geometrically in a variety of ways; however, the ^{13}C isotope effect depends almost exclusively on the C−O bond distance for the newly forming C−O bonds. All of the KIEs are within 0.004 of the quadratic trend line fitted to the data points; the absolute average deviation is 0.0007.

From this graph, the absolute experimental isotope effects correspond to C−O bond lengths of 2.11 Å and 2.26 Å. These bond lengths are in effect experimental transition-state geometries, though they will be subject to both random and systematic error. Random error arises from both the uncertainty in the experimental measurements and the imperfection of the C−O bond distance/KIE relationship. Using KIE uncertainties from a combination of the two sets of experimental values gives C−O bond lengths of 2.11 ± 0.03 Å and 2.26 ± 0.06 Å.

Systematic error is more difficult to handle in any measurement and could arise here either because the method for calculating isotope effects and tunneling corrections is systematically inaccurate or because the theoretical method systematically produces an incorrect relationship between the C−O distance and the ^{13}C KIE. Although there is no way to estimate the systematic error, there are two reasons to believe that it is not large. The first is that B3LYP calculations perform very well in modeling the oxidations of alkenes, giving a striking agreement between experimental and predicted KIEs for the epoxidation of 1-pentene with peracids,[8a] the asymmetric dihydroxylation of *t*-butylethylene,[8b] and the Shi epoxidation of *trans*-β-methylstyrene.[8d] The second, more notable reason is that the C−O bond distance/KIE relationship is theory-independent within limits to be discussed.

To examine the dependence of the C−O bond distance/KIE relationship on the calculational method, a diverse combination of functionals (RHF, B3LYP, BPW91, B3PW91, BP86, MPW1K, MPW3LYP, MPWLYP1M, BB1K, MPWB1K, MPW1B95, TPSS1KCIS, PBE1KCIS, PBE1W, PBELYP1W, TPSSLYP1W), basis sets (6-31G*, 6-31+G*, 6-31+G**, 6-311+G**), and solvent models (PCM and Onsager) was used to generate 60 distinct transition structures based on the previously proposed models (see the Supporting Information for the complete set of structures). As shown in Figure 5, the C−O bond distance/KIE relationship remains valid across a variety of calculational methods as long as the predicted activation barrier is reasonable (B3LYP, BPW91, B3PW91, BP86, MPW3LYP, MPWLYP1M, MPW1B95, TPSSKCIS, PBE1KCIS). Within the requirement that the calculation predicts the experimental rate within 4 orders of magnitude, the correlation between C−O bond distance and KIE is essentially independent of the basis set, solvent model, and functional.

Theoretical methods that gave calculated rates more than four orders of magnitude greater or less than experimental observations (based upon the free-energy barriers with the experimental conditions considered as the standard state) did not follow the relationship. For example, methods that overestimate the barrier of the reaction (such as MPW1K) led to a shift of the bond distance/KIE relationship to the left of the trend line (see the tables in the Supporting Information). The results here suggest that some caution should be taken with KIE calculations based on transition structures that do not correspond to an accurate barrier and that a good correlation of KIEs with structure should not be expected across theoretical methods that predict widely varying barriers.[6] The effect of barrier height may also be related to the lack of correlation between KIEs and geometrical parameters in literature studies that attempt to make correlations while significantly changing the electronics of the reaction.[12b,c]

(30) The set of 70 structures includes all possible transition states explored for the epoxidation of 2-methyl-2-butene catalyzed by 2-(methylsulfonyl)oxaziridine, *trans*-3-phenyl-2-methanesulfonyloxaziridine, and *cis*-3-phenyl-2-methanesulfonyloxaziridine calculated using B3LYP/6-31G*, B3LYP/6-31+G**, and B3LYP/6-311+G** in the gas phase, using an implicit Onsager solvent model, or using an implicit PCM solvent model.

We have previously emphasized the importance of applying tunneling corrections to the prediction of heavy-atom KIEs.[6] If a relationship analogous to that in Figure 5 were created without applying a tunneling correction to the prediction, the geometrical interpretation of a given KIE would correlate to a much shorter C−O bond distance. The error in bond distance increases with larger KIEs. For the experimental C2 KIE, the error in the bond distance would be 0.05 Å; this error increases to a maximum of 0.14 Å when the KIE is extrapolated to 1.040. This emphasizes the importance of applying tunneling corrections to heavy-atom KIEs, specifically in cases where the KIEs are greater than 1%.

This relationship allows a unique geometrical interpretation of the KIEs. The actual reaction is likely to involve an entire ensemble of low-energy transition structures, and the experimental KIEs reflect this ensemble. Therefore, a description of the transition state is not accurately represented by lowest-energy structure **7** alone. A more accurate description is derived from the average transition-state geometry of the ensemble using the C−O bond distance/KIE relationship from several structures.

To explore whether bond distance/KIE relationships can be established and used in another system, previously published results from a mechanistic study of the Shi epoxidation of β-methylstyrene were also examined.[8d] The Shi epoxidation (eq 2) is a good candidate for this process because a variety of transition structures arise from conformational isomerism in the catalyst in combination with multiple orientations for the approach of the alkene to the intermediate dioxirane.

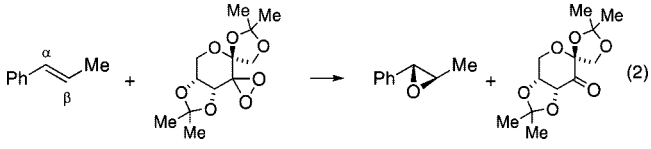

The transition state for the Shi epoxidation is spiro and asynchronous, as shown in the lowest-energy transition structure **13**. The previously calculated olefinic bond distances for the newly forming C−O bonds in structure **13** are 1.99 and 2.32 Å for the C_β−O and C_α−O bonds, respectively, and the predicted KIEs based on this structure were in excellent agreement with experimentally measured values. The relationship between the C−O bond distances and the KIEs was examined for 18 transition structures for the Shi epoxidation calculated using B3LYP/6-31G* (see the Supporting Information for the plot).[8d] As in the epoxidations with oxaziridines, a correlation between the C−O bond distances and the KIEs also exists for the Shi epoxidation. All of the KIEs are within 0.005 of a quadratic trend line fitted to the points; the absolute average deviation is 0.0018. From an average of the experimental KIE measurements, an average transition-state geometry of 1.99 and 2.38 Å for the C_β−O and C_α−O bond distances, respectively, can be derived from the relationship. The agreement between the best transition structure **13** and the average transition-state geometry derived from the relationship is remarkable, with errors of 0.00 and 0.06 Å for the C_β−O and C_α−O bond distances, respectively.

Analysis of KIE Predictions from Nonstationary Points. In the Schramm process, the inability of geometrically unconstrained optimizations from gas-phase calculations to mimic interactions with the enzyme necessitates the restriction of geometries in the frequency calculations; therefore, this method involves the prediction of KIEs from nonstationary points on the potential energy surface. On its face, this methodology appears dubious, since frequencies on which the isotope effect predictions depend are subject to intrinsic errors when calculated from nonstationary points.

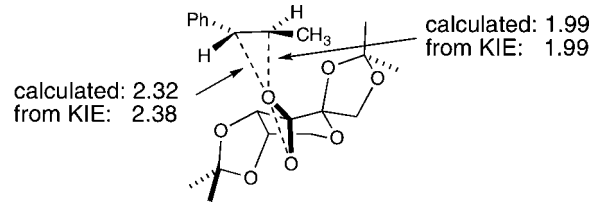

13

To evaluate the Schramm process, we examined how well it could define the distances of the forming C−O bonds in the transition structures for epoxidations with oxaziridines. This was done by first generating a grid of the predicted KIEs at C2 and C3 versus the distances of the forming C−O bonds from B3LYP/6-31G* calculations in the gas phase. This grid was based on structural analogues of **3** in which the C2−O and C3−O distances were fixed at 1.9−2.5 Å in 0.1 Å increments. The tunneling-corrected KIE predictions for 38 *nonstationary point* structures in this range were obtained on the basis of the Gaussian03-calculated frequencies, and interpolation was used to predict the KIEs for a total of 2800 geometries. The resulting grid was then used to translate the predicted KIEs based on 33 B3LYP *stationary points* (including both gas-phase and PCM-model structures) into the geometries expected for these structures. The deviation between the C−O distances obtained in this way and the actual C−O distances at the stationary points is a measure of the error induced by the Schramm process. In the event, the absolute average deviation for the 66 total distances is 0.05 Å, and the maximum error is 0.13 Å. It must be judged that the Schramm process is strikingly successful.

As expected, the largest deviations occur at longer C−O bond lengths (>2.3 Å), where very slight changes in the KIEs have a large effect on the bond distances. An average deviation of 0.04 Å reflects a systematic error that overpredicts the C−O bond distances. This systematic error is dominated by deviations of the fixed-distance geometries from stationary-point structures optimized with a PCM solvent model; this error could perhaps be reduced by exploring the use of other theoretical models as the parent structure for the fixed-parameter method. Using the grid to generate an estimate of the olefinic C−O bond lengths on the basis of the experimental KIEs for the reaction results in C−O bond distances within 0.03 and 0.08 Å for C3 and C2, respectively.

Why does the Schramm process work so well? When distances associated with bond forming or bond breaking are constrained at nonstationary points, the greatest errors in the resulting calculated frequencies should tend to occur in low-energy modes. Because the zero-point energy associated with such modes is small, their direct contribution to the KIEs is small. In addition, the frequencies calculated for isotopologues as part of the KIE-prediction process are based on an identical set of (likely flawed) force constants. As a result, errors in the calculated frequencies for isotopologues are related and tend to cancel out in the isotope effect prediction.[31]

The ability of nonstationary points to empirically predict transition structures is plausible since the contribution of low frequencies, which are incorrect in these constrained geometries, is small. Another possibility is that zero-point energies associated

(31) Schaad, L. J.; Bytautas, L.; Houk, K. N. *Can. J. Chem.* **1999**, *77*, 875–878.

with low frequencies tend to cancel out the effect of the low frequencies in the predictions. We cannot exclude the possibility that KIE predictions from nonstationary points may periodically contain errors associated with constrained motions at the transition state (see the Supporting Information for a discussion); however, these errors should be detectable in a grid of constrained transition-structure calculations.

Conclusions

Since KIEs are only significant when substantial bonding changes occur, the KIEs can never provide information about many aspects of the geometry at the transition state. However, they do provide information about the most important aspects of the geometry where bonds are being formed and broken. The work here supports the idea that the isotope effects can be used in a quantitative manner to define interatomic distances at transition states. The general procedure to be followed is to use calculations of model reactions to establish a relationship between KIEs and geometry, and the results here suggest that with care, such relationships can be independent of the theoretical method. Once such a relationship has been established, the experimental KIEs provide a specific measurement of the geometry. As with all measurements, there is some associated uncertainty; despite this limitation, the match between these experimentally based measurements and theoretical calculations can be remarkable. The precision in this methodology is sufficient to provide quantitative geometric insight into reaction mechanisms, and the methodology provides a quantitative picture that is not present in the usual qualitative interpretation of an experimental study.

The Schramm process accomplishes a similar quantitation of the transition-state geometry. The advantage of the Schramm methodology is that it can be applied to complex reactions where the energy surface provides no stationary-point models. The disadvantage is that the use of nonstationary points must inevitably introduce some degree of inaccuracy, but the results here suggest that the inaccuracies in the derived geometries are small, supporting its use in defining approximate transition-state geometries.

Experimental Section

Epoxidation of 2-Methyl-2-butene. To an ice-cooled solution of 31.3 g (120 mmol) of *trans*-2-(phenylsulfonyl)-3-phenyloxaziridine[32] in 70 mL of $CDCl_3$ was added slowly a solution of 10.5 g (150 mmol) of 2-methyl-2-butene in 10 mL of $CDCl_3$. After 48 h at room temperature, the reaction was found to be 77 ± 3% complete by ^{1}H NMR analysis of aliquots. The volatiles were then distilled from the reaction mixture using a 10 cm Vigreaux column until the head temperature reached 60 °C. The distillate was then redistilled fractionally to afford 1.1 g of the unreacted 2-methyl-2-butene (bp 35−38 °C, >99% pure by ^{1}H NMR). An analogous reaction under identical conditions was taken to 78 ± 3% conversion.

NMR Measurements. NMR measurements were taken on 1.1 g samples of 2-methyl-2-butene in 10 mm NMR tubes diluted with $CDCl_3$ to a constant height of 5 cm. A T_1 determination by the inversion−recovery method was carried out for each NMR sample, and T_1 for each NMR signal remained constant within experimental error from sample to sample. The ^{13}C spectra were recorded at 100.58 MHz with inverse gated decoupling, using 150 s delays between calibrated 45° pulses. An acquisition time of 7.301 s was used, and 262 144 points were collected. Integrations were determined numerically using a constant region for each peak that was ~5 times the peak width at half-height on either side of the peak. A zeroth-order baseline correction was generally applied, but in no case was a first order (tilt) correction applied. The results for all of the reactions are summarized in the Supporting Information.

Acknowledgment. We thank the NIH (GM-45617), NSF-CRIF (CHE-0541587), and The Robert A. Welch Foundation for support of this research.

Supporting Information Available: Energies and full geometries of all of the calculated structures, NMR integration results for all of the reactions, tables of KIEs versus C−O distances, a plot of KIEs versus C−O bond distance for the Shi epoxidation, a technical note on frequency calculations and KIE predictions, and complete ref 24a. This material is available free of charge via the Internet at http://pubs.acs.org.

JA8088636

(32) Davis, F. A.; Chattopadhyay, S.; Towson, J. C.; Lai, S.; Reddy, T. *J. Org. Chem.* **1988**, *53*, 2087–2089.